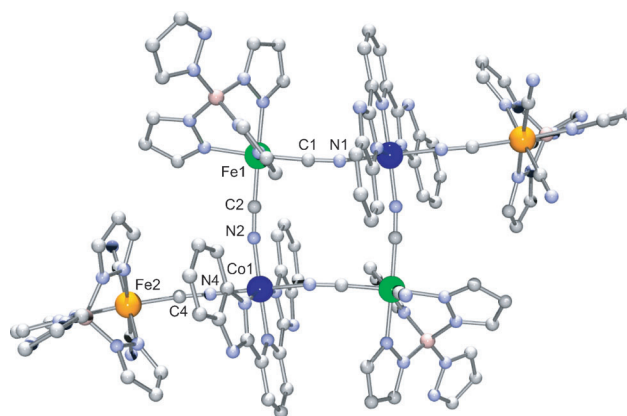


# A Light-Induced Phase Exhibiting Slow Magnetic Relaxation in a Cyanide-Bridged [Fe<sub>4</sub>Co<sub>2</sub>] Complex\*\*

Masayuki Nihei, Yuki Okamoto, Yoshihiro Sekine, Norihisa Hoshino, Takuya Shiga, Isiah Po-Chun Liu, and Hiroki Oshio\*

Since slow magnetic relaxation at low temperature for a dodecanuclear manganese cluster (Mn<sub>12</sub>) has been observed and this cluster was recognized as a single-molecule magnet (SMM), SMMs and single-chain magnets (SCMs) have been extensively studied in chemistry, physics, and materials science.<sup>[1]</sup> Light-responsive SMMs and SCMs have been one of the challenging target materials for potential applications in future molecular devices. In cyanide-bridged mixed-valence Fe–Co systems, light irradiation to the intervalence charge-transfer (IVCT) bands induces an electron transfer from the low-spin (LS) Fe<sup>II</sup> to the LS Co<sup>III</sup> ions, followed by the spin transition of the Co ions to the high-spin (HS) state, a process described as electron-transfer-coupled spin transition (ETCST).<sup>[2]</sup> A promising strategy for the construction of photoswitchable SMMs and SCMs is to introduce an ETCST-active chromophore, the photoinduced HS state of which should have uniaxial magnetic anisotropy, into a larger cluster molecule. Some cyanide-bridged multi-nuclear complexes have shown thermally and light-induced phase transitions accompanied with spin-state changes,<sup>[3]</sup> whereas in a cyanide-bridged coordination polymer, slow magnetic relaxation was observed in its photoinduced HS state.<sup>[4]</sup> Cyanide-bridged discrete system showing light-induced superparamagnetism have not been reported so far. We have recently reported a series of the cyanide-bridged molecular squares, one of which exhibited ETCST behavior.<sup>[5]</sup> Therefore, extended square systems may have a higher spin ground state and the uniaxial magnetic anisotropy, necessary for an SMM, and may also be expected to show light-switchable SMM behavior. We report here a cyanide-bridged extended square-type hexanuclear complex, [Co<sub>2</sub>Fe<sub>4</sub>(bimpy)<sub>2</sub>(CN)<sub>6</sub>(μ-CN)<sub>6</sub>(pztp)<sub>4</sub>]·2(1-PrOH)·4H<sub>2</sub>O (**1**) (bimpy = 2,6-bis(benzimidazol-2-yl)pyridine, pztp = tetrakis(1-pyrazolyl)borate), exhibiting a light-induced phase transition and slow magnetic relaxation (1-PrOH = 1-propanol).

In the previously reported [Fe<sub>2</sub>Co<sub>2</sub>] squares, the cobalt ions were capped by two bipyridine ligands.<sup>[5]</sup> The replacement of the two bipyridines with one tridentate ligand leaves one vacant coordination site on the cobalt ions, which is then available for the extension of the square. The reaction of (Bu<sub>4</sub>N)[Fe<sup>III</sup>(CN)<sub>3</sub>(pztp)] with Co(OTf)<sub>2</sub>·6H<sub>2</sub>O and bimpy in 1-PrOH yielded red tabular crystals of **1** (OTf = triflate = trifluoromethanesulfonate). X-ray crystallographic analyses of **1** were performed at 250 and 100 K (Figure 1; Table S1 in the Supporting Information), and the observed coordination



**Figure 1.** Molecular structure of **1** at 100 K. Solvent molecules and hydrogen atoms have been removed for clarity.

bond lengths are summarized in Table S2.<sup>[6]</sup> **1** crystallized in the triclinic space group *P* $\bar{1}$  with a complex molecule residing on the center of inversion. The central square core ([Co<sup>II</sup><sub>2</sub>Fe<sup>III</sup><sub>2</sub>)<sup>2+</sup>) is composed of alternately arranged [Fe(μ-CN)<sub>2</sub>(CN)(pztp)]<sup>−</sup> and [Co(bimpy)]<sup>2+</sup> units by the cyanide ligands, with two additional [Fe(μ-CN)(CN)<sub>2</sub>(pztp)]<sup>−</sup> units linked to the Co<sup>II</sup> ions of the square, forming the extended hexanuclear system [Fe<sup>III</sup>{Co<sup>II</sup><sub>2</sub>Fe<sup>III</sup><sub>2</sub>}Fe<sup>III</sup>].

In the square core, each Fe1 ion (see Figure 1) is coordinated by one tridentate pztp ligand and three cyanide carbon atoms, whereas the coordination sites of the Co ions are occupied by the tridentate bimpy and three cyanide nitrogen atoms. The peripheral Fe2 ions (see Figure 1) are coordinated by the tridentate pztp and the carbon atoms of three cyanide ions, one of which forms a bridge to the neighboring Co ion. At 250 K the average length of the coordination bond around the Co ion is 2.199(6) Å, characteristic of a HS Co<sup>II</sup> ion, whereas the average Fe–C<sub>CN</sub> and Fe–N<sub>pztp</sub> bond lengths are 1.921(8) and 1.959(6) Å for Fe1, and 1.908(8) and 1.965(6) Å for Fe2, respectively, which are

[\*] Dr. M. Nihei, Y. Okamoto, Y. Sekine, Dr. N. Hoshino, Dr. T. Shiga, Dr. I. P.-C. Liu, Prof. Dr. H. Oshio  
Graduate School of Pure and Applied Sciences  
University of Tsukuba, Tennodai 1-1-1, Tsukuba 305-8571 (Japan)  
E-mail: oshio@chem.tsukuba.ac.jp

[\*\*] This work was supported by a Grant-in-Aid for Scientific Research on Innovative Areas ("Coordination Programming" Area 2107, No. 21108006) from the Ministry of Education, Culture, Sports, Science and Technology (Japan) and by the KEK (grant number 10K0028).

Supporting information for this article is available on the WWW under <http://dx.doi.org/10.1002/anie.201202225>.

typical values for LS Fe<sup>II</sup> or LS Fe<sup>III</sup> ions. <sup>57</sup>Fe Mössbauer spectra (see Figure S1 in the Supporting Information) revealed that both Fe1 and Fe2 are LS Fe<sup>III</sup> ions at 250 K. The X-ray structural data at 100 K suggested an electronic state transition had occurred with the temperature change. At 100 K, the average coordination bond length around Co1 is 1.928(3) Å, characteristic of a LS Co<sup>III</sup> ion. The average Fe1–C<sub>CN</sub> and Fe1–N<sub>pzt</sub> bond lengths at 100 K also showed changes from those at 250 K. The bond length changes between 250 and 100 K were  $\Delta_{\text{Fe1-C}} = 0.037(8)$  Å and  $\Delta_{\text{Fe1-N}} = +0.034(6)$  Å, while the coordination bond lengths of the Fe2 ion showed small changes ( $\Delta_{\text{Fe2-C}} = 0.014(8)$  Å and  $\Delta_{\text{Fe2-N}} = +0.014(6)$  Å) upon decreasing temperature. The structural changes around the Fe1 ion suggested that its electronic state had changed to LS Fe<sup>II</sup>, whereas the Fe2 ion had remained LS Fe<sup>III</sup> at 100 K. The oxidation states of the Fe ions were confirmed by Mössbauer measurements. The <sup>57</sup>Fe Mössbauer spectra (Figure S1 in the Supporting Information) were recorded at 100 and 250 K and the parameters are summarized in Table S3. The Mössbauer spectrum at 250 K in the high-temperature phase showed two quadrupole doublets, of which the parameters ( $\delta = -0.08$  and  $\Delta E_Q = 0.98$  mm s<sup>-1</sup>, and  $\delta = 0.03$  and  $\Delta E_Q = 1.01$  mm s<sup>-1</sup>) were characteristic of LS Fe<sup>III</sup> ions. In contrast a new doublet appeared at 100 K, replacing one LS Fe<sup>III</sup> doublet, and the peak area ratio of the new doublet to that of the remaining LS Fe<sup>III</sup> species was 0.48:0.52. The new doublet could be assigned to a LS Fe<sup>II</sup> species from the Mössbauer parameters ( $\delta = 0.16$  and  $\Delta E_Q = 0.50$  mm s<sup>-1</sup>). The Mössbauer data suggested that the electronic states of **1** were [Fe<sup>III</sup><sub>LS</sub>{Co<sup>II</sup><sub>HS2</sub>Fe<sup>III</sup><sub>LS2</sub>}Fe<sup>III</sup><sub>LS</sub>] and [Fe<sup>III</sup><sub>LS</sub>{Co<sup>III</sup><sub>LS2</sub>Fe<sup>II</sup><sub>LS2</sub>}Fe<sup>III</sup><sub>LS</sub>] at 250 and 100 K, respectively, constituting the high-temperature (HT) and low-temperature (LT) phases, in agreement with the X-ray structural data. It was concluded that **1** exhibited thermal ETCST behavior associated with two electron-transfer processes between the Co and Fe ions in the central square core.

The ETCST behavior in **1** was confirmed by direct current (dc) magnetic susceptibility measurements in the temperature range of 5 to 270 K (Figure 2). The  $\chi_m T$  values ( $\chi_m$  = molar susceptibility) were nearly constant down to 250 K, followed by a gradual decrease centered around 220 K, because of the occurrence of ETCST from the HT phase to the LT phase in this temperature range. The  $\chi_m T$  value was 8.12 emu mol<sup>-1</sup> K in the HT phase at 270 K, close to the Curie constant (8.13 emu mol<sup>-1</sup> K) calculated for uncorrelated four LS Fe<sup>III</sup>

( $S = 1/2$ ,  $g_{\text{Fe}} = 2.7$ ) and two HS Co<sup>II</sup> ( $S = 3/2$ ,  $g_{\text{Co}} = 2.4$ ) ions. The large  $g$  values agree with those reported for correlated Fe<sup>III</sup> and Co<sup>II</sup> complexes.<sup>[3c,7]</sup> In the LT phase the plateau value (1.44 emu mol<sup>-1</sup> K at 100 K) corresponds to the theoretical value (1.37 emu mol<sup>-1</sup> K) expected for two magnetically isolated LS Fe<sup>III</sup> ions. The ETCST behavior in **1** was fully reversible in the temperature range of 5–270 K.

Light irradiation experiments were performed on **1** at 5 K in the superconducting quantum interference device (SQUID) magnetometer, where the microcrystalline sample fixed in a transparent polymer matrix was used to avoid crystal alignment by the applied magnetic field (Figure 2). Cyanide-bridged complexes with Fe<sup>II</sup><sub>LS</sub>-CN-Co<sup>III</sup><sub>LS</sub> units have been shown to exhibit a broad absorption band at about 750 nm, assignable to an Fe<sup>II</sup>→Co<sup>III</sup> IVCT transition.<sup>[5,8]</sup> A 808 nm laser light was, therefore, used for the irradiation experiments. A significant increase in the  $\chi_m T$  value was observed upon light irradiation at 5 K, reaching a saturation value of 20.31 emu mol<sup>-1</sup> K after irradiation for 150 min. As the temperature was raised after turning off the laser light, the  $\chi_m T$  values decreased to a plateau at 66 K, followed by a sudden decrease to the  $\chi_m T$  value of 1.49 emu mol<sup>-1</sup> K at 130 K. The temperature dependence of the  $\chi_m T$  values suggested the occurrence of intra- and/or intermolecular ferromagnetic interactions in the photoinduced (HT\*) phase, before the HT\* phase thermally relaxed back to the LT phase at 130 K. X-ray data were collected at 20 K before and after the light irradiation, to obtain information about the structural changes upon light irradiation (see Tables S1 and S2 in the Supporting Information). The average coordination bond lengths before the irradiation were 1.94(1), 1.94(1), and 1.933(9) Å for Fe1, Fe2, and Co ions, respectively, supporting its assignment as the [Fe<sup>III</sup><sub>LS</sub>{Co<sup>III</sup><sub>LS2</sub>Fe<sup>II</sup><sub>LS2</sub>}Fe<sup>III</sup><sub>LS</sub>] electronic state. After the irradiation no change in the space group was observed, however, the coordination bond lengths differed from those in the LT phase. The average coordination bond lengths of the Fe1, Fe2 and Co ions were 1.94(1), 1.93(1), and 2.04(1) Å, respectively, close to the values observed for the HT phase. The bond length changes ( $\Delta_{\text{Fe1-C}} = 0.03(1)$  Å and  $\Delta_{\text{Fe1-N}} = 0.03(1)$  Å, and  $\Delta_{\text{Fe2-C}} = 0.01(1)$  Å and  $\Delta_{\text{Fe2-N}} = 0.03(3)$  Å) were not significantly different, which may be due to incomplete light-induced phase transition. The electronic state of the photoinduced high-spin (HT\*) phase was understood to be [Fe<sup>III</sup><sub>LS</sub>{Co<sup>II</sup><sub>HS2</sub>Fe<sup>III</sup><sub>LS2</sub>}Fe<sup>III</sup><sub>LS</sub>], the same as the HT phase, resulting from two electron-transfer processes in the square core.

The field dependence of the magnetization was recorded at 1.8 K before and after light irradiation (Figure S2 in the Supporting Information). The magnetization values significantly increased with light irradiation, suggesting the generation of a species with a higher spin ground state. The saturation value of magnetization at 5 T was 2.09 N $\beta$  before light irradiation, corresponding to the value expected for two isolated LS Fe<sup>III</sup> species in the LT phase. On the other hand, in the light-induced HT\* phase the magnetization showed a rapid increase at lower magnetic fields, followed by a gradual increase to 6.8 N $\beta$  at 5 T. At sufficiently low temperature a Co<sup>II</sup> ion may be treated as an effective spin of  $S' = 1/2$  with anisotropic  $g'$  values,<sup>[9]</sup> and the spin ground state of **1** in the

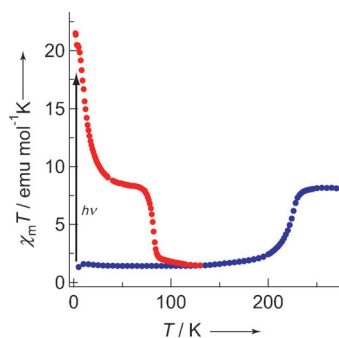


**Figure 2.** Plots of  $\chi_m T$  versus  $T$  for **1** before (blue) and after (red) light irradiation.

light-induced HT\* phase can thus be  $S=3$ , due to intramolecular ferromagnetic interactions.

Some reported cyanide-bridged  $\text{Fe}^{\text{III}}\text{--Co}^{\text{II}}$  complexes have exhibited intramolecular ferromagnetic interactions,<sup>[10]</sup> and the HT\* phase in **1** replicated this behavior. The  $\chi_{\text{m}}T$  value of the HT\* phase was  $21.50 \text{ emu mol}^{-1} \text{ K}$  at 1.8 K, which was higher than the value ( $11.20 \text{ emu mol}^{-1} \text{ K}$ ) calculated for an  $S=3$  species with  $g_{\text{Fe}}=2.1$  and  $g_{\text{Co}}=4.0$ . This implies that the intermolecular interactions are also ferromagnetic. The structural analyses for the HT\* phase revealed close intermolecular contacts (a N5...C34 distances of  $3.635 \text{ \AA}$ ) between a cyanide nitrogen atom of the peripheral  $[\text{Fe}(\text{CN})_3(\text{pztp})]^-$  unit and a pyridine ring in the bipy ligand (Figure S3 in the Supporting information). DFT calculations for the  $[\text{Fe}(\text{CN})_3(\text{pztp})]^-$  and  $[\text{Co}(\text{bimpy})_2(\text{NC})_3]^-$  units suggested that the terminal cyanide nitrogen atom (N5) has a positive spin density, whereas the pyridine carbon atom (C34) in the bimpy has a negative spin density. The close contact of the N5 and C34\* atoms may be responsible for the occurrence of the intermolecular ferromagnetic interactions. As previously reported, a structurally related cyanide-bridged  $[\text{Fe}^{\text{III}}_2\text{Ni}^{\text{II}}_2]$  square showed both intra- and intermolecular ferromagnetic interactions, and the latter were explained by the spin polarization of  $\pi$ -stacked ligands.<sup>[11]</sup> The  $\chi_{\text{m}}T$  value ( $=8.26 \text{ emu mol}^{-1} \text{ K}$ ) at 66 K in the HT\* phase was close to the value ( $8.12 \text{ emu mol}^{-1} \text{ K}$ ) in the HT phase at 270 K, suggesting that the transformation from the LT phase to the HT\* phase was essentially complete, in contrast to the incomplete photoinduced phase transition observed in the single-crystal X-ray experiments. Zero-field-cooled and field-cooled magnetization measurements under  $H_{\text{ext}}=15 \text{ Oe}$  showed no bifurcation down to 1.8 K, suggesting that the blocking temperature of the ferromagnetic ordering is lower than 1.8 K (Figure S4 in the Supporting Information).

Alternating current (ac) magnetic susceptibility measurements were carried out before and after light irradiation under an ac magnetic field ( $H_{\text{ac}}$ ) of 3 Oe oscillating at 10–1500 Hz and an external dc field ( $H_{\text{ext}}$ ) of 0–1000 Oe. No frequency dependence was observed before irradiation (see Figure S5 in the Supporting Information). In contrast, frequency-dependent in-phase ( $\chi_{\text{m}}'$ ) and out-of-phase ( $\chi_{\text{m}}''$ ) signals were observed after light irradiation, although no peak maxima of  $\chi_{\text{m}}''$  were detected in the temperature range measured when  $H_{\text{ext}}=0 \text{ Oe}$  (Figure S6 in the Supporting Information). Since it has been reported that the energy barrier ( $\Delta E$ ) of magnetization reversal in SMMs can be tuned by applying  $H_{\text{ext}}$ ,<sup>[12]</sup> the ac susceptibility measurements were recorded with  $H_{\text{ext}}=250\text{--}1000 \text{ Oe}$  (Figure S7 in the Supporting Information). In the ac magnetic data at  $H_{\text{ext}}=500 \text{ Oe}$ , both the  $\chi_{\text{m}}'$  and  $\chi_{\text{m}}''$  signals showed peak maxima shifting to higher temperature with increasing ac field frequency, characteristic of slow magnetic relaxations (Figure 3). Cole–Cole plots obtained from the data with  $H_{\text{ext}}=500 \text{ Oe}$  were analyzed by the generalized Debye model (Figure S8 in the Supporting Information), and an  $\alpha$  value of 0.20–0.34 was obtained (Table S4), suggesting mono-dispersibility of magnetic relaxations.<sup>[13]</sup>

In summary, thermal and light-induced ETCST have been investigated in the cyanide-bridged hexanuclear complex **1**.

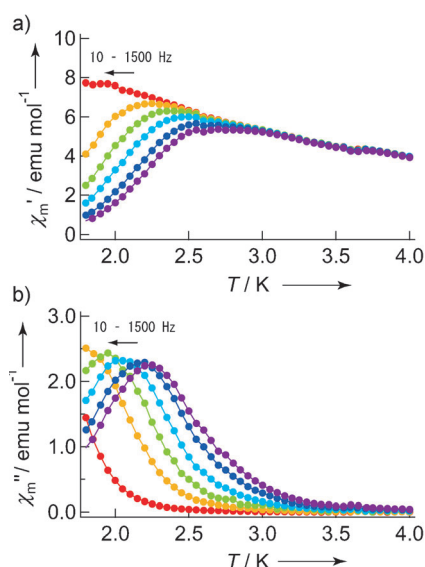


**Figure 3.** Plots of a)  $\chi_{\text{m}}'$  versus  $T$  and b)  $\chi_{\text{m}}''$  versus  $T$  for **1** after light irradiation with  $H_{\text{ac}}=3 \text{ Oe}$  oscillating at 10–1500 Hz and  $H_{\text{ext}}=500 \text{ Oe}$ .

The light-induced HT\* phase showed slow magnetic relaxation characteristic of superparamagnetism, the first observation of such synergic behavior in a discrete molecule.

## Experimental Section

**Synthesis:** All reagents were obtained from commercial suppliers and were used without further purification.  $\text{Co}(\text{OTf})_2 \cdot 6\text{H}_2\text{O}$ ,  $(\text{Bu}_4\text{N})[\text{Fe}(\text{CN})_3(\text{Htp})]$ ,  $(\text{Bu}_4\text{N})[\text{Fe}(\text{CN})_3(\text{pztp})]$ , and bimpy were prepared according to the literature methods.<sup>[14–16]</sup>

The reaction of bimpy (6 mg, 0.020 mmol) with  $\text{Co}(\text{OTf})_2 \cdot 6\text{H}_2\text{O}$  (7 mg, 0.015 mmol) in 1-PrOH (10 mL) gave a pale yellow solution. To the solution was added  $(\text{Bu}_4\text{N})[\text{Fe}(\text{CN})_3(\text{pztp})]$  (20 mg, 0.030 mmol) in 1-PrOH (2 mL), and after stirring for 5 min the reaction mixture was filtered. The filtrate was allowed to stand for 1 day to give red tabular crystals of **1**. (10 mg, 0.0038 mmol, yield of 50%) Anal. Calcd. for  $\text{C}_{104}\text{H}_{98}\text{B}_4\text{Co}_2\text{Fe}_4\text{N}_{24}\text{O}_6$ : C, 48.33; H, 3.82; N, 29.26%. Found: C, 48.06; H, 3.79; N, 28.93%. IR (KBr):  $\tilde{\nu}=2168$  ( $\nu_{\text{CN}}$ ), 2152 ( $\nu_{\text{CN}}$ ), 2135 ( $\nu_{\text{CN}}$ ), and 2125  $\text{cm}^{-1}$  ( $\nu_{\text{CN}}$ ).

Received: March 21, 2012

Published online: May 3, 2012

**Keywords:** cobalt · cyanides · heterometallic complexes · iron · mixed-valent compounds

- [1] a) D. Gatteschi, R. Sessoli, J. Villain, *Molecular Nanomagnets*, Oxford University Press, New York, **2006**; b) D. Gatteschi, R. Sessoli, *Angew. Chem.* **2003**, *115*, 278; *Angew. Chem. Int. Ed.* **2003**, *42*, 268; c) H. Oshio, M. Nakano, *Chem. Eur. J.* **2005**, *11*, 5178; d) C. Coulon, H. Miyasaka, R. Clérac, *Struct. Bonding (Berlin)* **2006**, *122*, 163.
- [2] G. N. Newton, M. Nihei, H. Oshio, *Eur. J. Inorg. Chem.* **2011**, 3031.
- [3] a) C. P. Berlinguette, A. Dragulescu-Andrasi, A. Sieber, J. R. Galán-Mascarós, H.-U. Güdel, C. Achim, K. R. Dunbar, *J. Am. Chem. Soc.* **2004**, *126*, 6222; b) C. P. Berlinguette, A. Dragulescu-Andrasi, A. Sieber, H.-U. Güdel, C. Achim, K. R. Dunbar, *J.*

- Am. Chem. Soc.* **2005**, *127*, 6766; c) D. Li, R. Clérac, O. Roubeau, E. Harté, C. Mathonière, R. L. Bris, S. M. Holmes, *J. Am. Chem. Soc.* **2008**, *130*, 252; d) Y. Zhang, D. Li, R. Clérac, M. Kalisz, C. Mathonière, S. M. Holmes, *Angew. Chem.* **2010**, *122*, 3840; *Angew. Chem. Int. Ed.* **2010**, *49*, 3752; e) M. G. Hilfiger, M. Ghen, T. V. Brinzari, M. Nocera, M. Shatruk, D. T. Petasis, J. L. Musfeldt, C. Achim, K. R. Dunbar, *Angew. Chem.* **2010**, *122*, 1452; *Angew. Chem. Int. Ed.* **2010**, *49*, 1410; f) M. Nihei, Y. Sekine, N. Suganami, H. Oshio, *Chem. Lett.* **2010**, *39*, 978; g) K. Mitsumoto, E. Oshiro, H. Nishikawa, T. Shiga, Y. Yamamura, K. Saito, H. Oshio, *Chem. Eur. J.* **2011**, *17*, 9612; h) K. E. Funck, A. V. Prosvirin, C. Mathonière, R. Clérac, K. R. Dunbar, *Inorg. Chem.* **2011**, *50*, 2782; i) J. Mercurol, Y. Li, E. Pardo, O. Risset, M. Seuleiman, H. Rousselière, R. Lescouëzec, M. Julve, *Chem. Commun.* **2010**, *46*, 8995.
- [4] T. Liu, Y.-J. Zhang, S. Kanegawa, O. Sato, *J. Am. Chem. Soc.* **2010**, *132*, 8250.
- [5] M. Nihei, Y. Sekine, N. Suganami, K. Nakazawa, A. Nakao, H. Nakao, Y. Murakami, H. Oshio, *J. Am. Chem. Soc.* **2011**, *133*, 3592.
- [6] Crystal structure data for **1** at 250 K:  $C_{104}H_{98}B_4Co_2Fe_4N_{54}O_6$ , triclinic  $P\bar{1}$ ,  $a = 12.556(6)$ ,  $b = 14.093(6)$ ,  $c = 18.158(8)$  Å,  $\alpha = 73.463(6)$ ,  $\beta = 70.170(6)$ ,  $\gamma = 85.044(6)^\circ$ ,  $V = 2897(2)$  Å<sup>3</sup>,  $Z = 1$ ,  $d_{\text{calcd.}} = 1.482$  g cm<sup>-3</sup>, final  $R1 = 0.0650$ ,  $wR2 = 0.1233$ ; at 100 K: triclinic  $P\bar{1}$ ,  $a = 12.287(5)$ ,  $b = 13.963(5)$ ,  $c = 17.757(7)$  Å,  $\alpha = 72.968(4)$ ,  $\beta = 69.944(5)$ ,  $\gamma = 69.944(5)^\circ$ ,  $V = 2736(2)$  Å<sup>3</sup>,  $Z = 1$ ,  $d_{\text{calcd.}} = 1.569$  g cm<sup>-3</sup>, final  $R1 = 0.0567$ ,  $wR2 = 0.1482$ ; at 20 K: triclinic  $P\bar{1}$ ,  $a = 12.252(8)$ ,  $b = 13.877(9)$ ,  $c = 17.61(1)$  Å,  $\alpha = 73.152(9)$ ,  $\beta = 70.433(8)$ ,  $\gamma = 84.950(9)^\circ$ ,  $V = 2700(3)$  Å<sup>3</sup>,  $Z = 1$ ,  $d_{\text{calcd.}} = 1.590$  g cm<sup>-3</sup>, final  $R1 = 0.0923$ ,  $wR2 = 0.1965$ ; at 20 K after irradiation: triclinic  $P\bar{1}$ ,  $a = 12.34(1)$ ,  $b = 13.96(1)$ ,  $c = 17.82(2)$  Å,  $\alpha = 73.24(1)$ ,  $\beta = 70.21(1)$ ,  $\gamma = 85.40(1)^\circ$ ,  $V = 2765(4)$  Å<sup>3</sup>,  $Z = 1$ ,  $d_{\text{calcd.}} = 1.553$  g cm<sup>-3</sup>, final  $R1 = 0.1063$ ,  $wR2 = 0.2189$ . CCDC 871861, 871862, 871863, 871864 contain the supplementary crystallographic data for this paper. These data can be obtained free of charge from The Cambridge Crystallographic Data Centre via [www.ccdc.cam.ac.uk/data\\_request/cif](http://www.ccdc.cam.ac.uk/data_request/cif).
- [7] a) A. T. Casey, S. Mitra in *Theory and Applications of Molecular Paramagnetism, Vol. 1* (Eds.: E. A. Boudreaux, L. N. Mulay), Wiley, New York, **1976**, pp. 190–195; b) J. Kim, S. Han, K. I. Pokhodnya, J. M. Migliori, J. S. Miller, *Inorg. Chem.* **2005**, *44*, 6983.
- [8] P. V. Bernhardt, F. Bozoglian, B. P. Macpherson, M. Martínez, *Coord. Chem. Rev.* **2005**, *249*, 1902.
- [9] O. Kahn, *Molecular Magnetism*, VCH, Weinheim, **1993**, p. 38.
- [10] a) R. Lescouëzec, J. Vaissermann, C. Ruiz-Pérez, F. Lloret, R. Carrasco, M. Julve, M. Verdaguer, Y. Dromzee, D. Gatteschi, W. Wernsdorfer, *Angew. Chem.* **2003**, *115*, 1521; *Angew. Chem. Int. Ed.* **2003**, *42*, 1483; b) L. Jiang, H. J. Choi, X.-L. Feng, T.-B. Lu, J. R. Long, *Inorg. Chem.* **2007**, *46*, 2181.
- [11] E. Pardo, M. Verdaguer, P. Herson, H. Rousselière, J. Cano, M. Julve, F. Lloret, R. Lescouëzec, *Inorg. Chem.* **2011**, *50*, 6250.
- [12] S. M. J. Aubin, N. R. Dilley, L. Pardi, J. Krzystek, M. W. Wemple, L.-C. Brunel, M. B. Maple, G. Christou, D. N. Hendrickson, *J. Am. Chem. Soc.* **1998**, *120*, 4991.
- [13] K. S. Cole, R. H. Cole, *J. Chem. Phys.* **1941**, *9*, 341.
- [14] S. H. John, R. S. John, C. T. Robwer, *Can. J. Chem.* **1981**, *59*, 669.
- [15] Z. Gu, W. Liu, Q. Yang, X. Zhou, J. Zuo, X. You, *Inorg. Chem.* **2007**, *46*, 3236.
- [16] S. Yue, H. Xu, J. Ma, Z. Su, Y. Kan, H. Zhang, *Polyhedron* **2006**, *25*, 635.